Am J Nucl Med Mol Imaging 2013;3(3):217-231
www.ajnmmi.us /ISSN:2160-8407/ajnmmi1302004

Review Article

Intravascular near-infrared fluorescence molecular imaging of atherosclerosis

Arun K Thukkani[1], Farouc A Jaffer[2]

[1]*Cardiovascular Division, Brigham and Women's Hospital, Harvard Medical School, 70 Francis Street, Boston, MA 02115, USA;* [2]*Massachusetts General Hospital, Harvard Medical School, Cardiovascular Research Center, 185 Cambridge Street, Room 3206, Boston, Massachusetts 02114, USA*

Received February 21, 2013; Accepted March 11, 2013; Epub April 9, 2013; Published April 15, 2013

Abstract: Novel imaging modalities are required to better identify vulnerable atherosclerotic plaques before their dire consequences of myocardial infarction, sudden death, and stroke. Moving beyond traditional diagnostic methods, the field of molecular imaging offers an innovative approach to report upon critical *in vivo* biological features of high-risk plaques. Molecular imaging employs engineered, targeted imaging agents in conjunction with sophisticated, high-resolution detection systems. While various modalities have been investigated for this purpose, intravascular near infrared fluorescence imaging (NIRF) strategies are uniquely poised to provide high-resolution readouts of human coronary artery plaques. To date, preclinical animal studies have demonstrated feasibility of both standalone NIRF intravascular imaging as well as dual-modality approaches detecting inflammation and fibrin deposition in coronary-sized arteries. This translatable catheter-based approach is positioned to advance the identification of biologically vulnerable coronary plaques and coronary stents at risk of thrombosis.

Keywords: Near-infrared intravascular imaging, atherosclerosis, coronary, vulnerable plaque, inflammation, coronary stenting

Introduction

Atherosclerosis remains a major cause of morbidity and mortality in both industrialized and developing countries. Despite advances in medical, interventional, and surgical treatments, the proportion of healthcare expenditures dedicated to atherosclerotic vascular disease continues to accrue [1, 2]. Accordingly, there remains a pressing need to develop diagnostic imaging systems that accurately and sensitively detect high-risk or "vulnerable" atherosclerotic plaques. If such plaques can be detected prior to becoming clinically evident, intensified pharmacological or mechanical interventions could be initiated preemptively. In this way, the devastating and costly complications of sudden cardiac death, myocardial infarction, and stroke stemming from plaque rupture may be prevented.

For the last several decades, x-ray angiography of luminal stenosis severity has remained the primary diagnostic modality guiding coronary arterial risk assessment. While widely adopted in clinical practice, several lines of evidence have collectively suggested that angiography used in isolation may not be ideal for risk prediction. For example, as early atherosclerotic plaques develop, they typically undergo positive remodeling, where plaque expansion is outward and does not compromise the luminal area [3]. Consequently, while luminal angiography may only demonstrate a mild or moderate stenosis, a relatively large, eccentric, and potentially vulnerable lesion may reside in the arterial wall. Several autopsy series support this notion, as the majority of plaques responsible for fatal myocardial infarctions arise from plaques of only moderate angiographic severity [4]. Coupled with clinical studies demonstrating cardiovascular mortality rates are unchanged despite intervening on angiographically severe lesions, it is clear that new diagnostic modalities are needed to identify high-risk plaques that will cause heart attack, stroke, and death [5].

Spurred by advances in molecular biology, synthetic chemistry, materials science, and multimodal diagnostic imaging over the last decade, the field of cardiovascular molecular imaging has emerged to address this need. By utilizing sensitive molecular and cellular imaging agents that can be detected by various imaging platforms, *in vivo* molecular imaging is significantly impacting preclinical cardiovascular molecular imaging research and early clinical trials [6-8]. Destabilizing processes in atherosclerotic lesions such as inflammation, oxidative stress, and apoptosis are now detectable via specialized optical, magnetic resonance (MR), ultrasound, and positron emission tomography (PET) molecular imaging agents. While clinical translation of these approaches is still in early phases, it is anticipated that molecular imaging will augment contemporary risk stratification paradigms typically based on plaque burden. By more precisely gauging individual cardiovascular risk, medical and interventional therapy could be tailored and more optimally applied. In this review, we focus on molecular imaging approaches with high translatability to the human coronary artery, the arterial bed responsible for myocardial infarction and sudden cardiac death.

Biological framework

Atherosclerosis is a chronic lipid- and inflammation-driven arteriopathy leading to the development of obstructive plaques in the coronary, cerebral, and peripheral medium-to-large sized arteries [9]. Triggered by lipid deposition and oxidation in the vessel wall, activated endothelial cells attract circulating monocytes that then transform into activated plaque macrophages, the key inflammatory cellular mediator in atherosclerosis. Macrophages in this initial fatty streak then undergo apoptosis and necrosis, leading to the development of a necrotic core. In addition, plaque macrophages release intracellular lipids, cytokines, and destructive proteases that may expand the burgeoning atheroma. Activated matrix metalloproteinases (MMPs), serine proteases, and cysteine proteases destabilize the critical fibrous cap by degrading key extracellular matrix components such as collagen and elastin [10]. In particular, histologic studies of inflamed plaques demonstrate overexpression of cathepsins, a family of lysosomal cysteine proteases that are a major target of NIRF imaging agents [11]. Persistent inflammation and proteolysis lead to the development of a thin-capped fibroatheroma (TCFA), the prototypical high-risk, unstable lesion that is believed to undergo plaque rupture. Plaque rupture and release of its highly thrombogenic constituents into the bloodstream provokes acute thrombotic arterial occlusion, leading to myocardial infarction, sudden cardiac death, or stroke. The well-developed biological framework of atheroma progression has provided a rich array of high-value targets suitable for *in vivo* molecular imaging of atherosclerosis in animals and in large vessels of patients [6-8]. Only recently has substantial effort been focused on molecular imaging of coronary artery disease.

Clinical atherosclerosis molecular imaging

Over the last decade, innovative imaging approaches have illuminated multiple features of atheroma inflammation in larger-sized arteries of clinical subjects. The first major advance in this field utilized USPIO (ultrasmall superparamagnetic iron oxides, e.g. ferumoxtran or ferumoxytol) to enable high-resolution MRI of carotid plaque macrophage accumulation, and to report on macrophage modulation following statin therapy [12-14]. To date, these studies have focused upon the imaging of larger, relatively immobile arteries such as the carotid arteries or aorta. Due to its limited temporal resolution, high-resolution MR imaging of smaller plaques in the much more mobile coronary arteries is a significant challenge.

The second major advance in the field of clinical atherosclerosis molecular imaging occurred by Rudd et al. in 2002 when the metabolic PET reporter agent ^{18}F-FDG was used to noninvasively image plaque macrophages in larger arteries [15, 16]. With widespread availability, ^{18}F-FDG PET has been traditionally utilized for oncologic imaging. Notably, ^{18}F-FDG PET imaging of atherosclerosis has been described and was utilized in a recent clinical trial assessing the effects of dalcetrapib, an investigational pharmaceutical, on human atheroma [17]. ^{18}F-FDG PET atheroma imaging may therefore greatly aid the field of cardiovascular drug discovery. ^{18}F-FDG PET imaging of atherosclerotic vascular inflammation has been demonstrated in the human coronary artery, though at lower

resolution, as well [18, 19]. However, several challenges limit the wider use of ^{18}F-FDG PET to image inflamed human coronary arteries. For example, despite diet-based suppressive protocols that limit background myocardial uptake of ^{18}F-FDG, a substantial percentage of coronary arterial segments remain uninterepretable [20]. Currently, standardized protocols for atherosclerosis PET imaging are not yet available [21]. In addition to overcome motion-induced artifacts and blurring, cardiac gating protocols could constrain image acquisition to diastole, but would further diminish sensitivity due the extended time needed for acquisition and the limited half-life of ^{18}F. These limitations have spurred investigation into alternative approaches to image coronary arterial inflammation. In the following sections, we review a new translational approach utilizing intravascular near-infrared fluorescence (NIRF) molecular imaging to image arterial inflammation at high-resolution in coronary sized arteries.

NIRF imaging

Fluorescence-based molecular imaging approaches offer high-resolution, good sensitivity, and versatile detection of investigational targets in both preclinical and clinical cardiovascular disease [22]. NIRF imaging has recently emerged as a sensitive, high-resolution approach for *in vivo* atherosclerotic molecular imaging without the use of ionizing radiation. For *in vivo* imaging, the NIR window (700-900nm) is particularly favorable compared to other wavelengths, as this window demonstrates reduced blood attenuation of light and reduced autofluorescence [23]. The NIR window is therefore favorable for molecular imaging of human coronary artery-sized vessels (i.e. 2.5-4.0mm in diameter), particularly through blood [24].

Molecular imaging agents for NIRF inflammation imaging

Leveraging an array of smart activatable agents and/or nanomaterials, enhanced atherosclerotic proteolytic activity [25], macrophage-mediated inflammation [26], endothelial adhesion molecule surface expression [27], and thrombin activity [28, 29] have all been imaged *in vivo* using NIRF molecular imaging approaches.

Intravascular NIRF imaging

Optical imaging has produced major advances in clinical intracoronary imaging in the last decade, with FDA approval of intravascular optical coherence tomography (OCT) catheters and near-infrared spectroscopy (NIRS) catheters. As NIRF is also a light-based approach, new imaging systems applicable to the human coronary artery can be developed exploiting flexible optical fibers. Recently, intravascular NIRF detection catheters have been developed for *in vivo* vascular imaging. These novel imaging platforms have been used in conjunction with protease-activatable NIRF imaging agents for preclinical research and will likely aid in both investigating *in vivo* plaque inflammation as well as elucidating the temporal-spatial patterns of the arterial healing response to injury following balloon angioplasty and stent implantation [24, 30]. Moreover, NIRF imaging catheters have also been engineered with optical frequency domain imaging (OFDI) capability [22]. Thus, *in vivo* NIRF-derived molecular signals can be readily integrated with microstructural imaging of the stent-artery interface in order to provide precise anatomic correlation to stent-associated inflammatory injury and fibrin deposition patterns. Overall, intravascular NIRF molecular imaging is positioned to address important yet currently unmet clinical needs by detecting the *in vivo* biomolecular features associated with vulnerable plaques. Additionally, such a tool may also help identify patients with previously implanted stents that are at greater risk for developing stent thrombosis or restenosis, both major causes of cardiovascular morbidity and mortality.

In vivo intravascular NIRF molecular imaging of atherosclerosis

Imaging cysteine protease activity in inflamed atheroma

Via degradation of the collagen-rich fibrous caps, enhanced plaque proteolytic activity is mechanistically linked to plaque rupture. In particular, post-mortem histological studies demonstrate significantly elevated expression of cathepsins S and K particularly at the sites of overt plaque rupture [11]. Cathepsin B is another cysteine protease implicated in the pathogenesis of atherosclerosis [31]. In conjunction, these findings indicate that cathepsins demar-

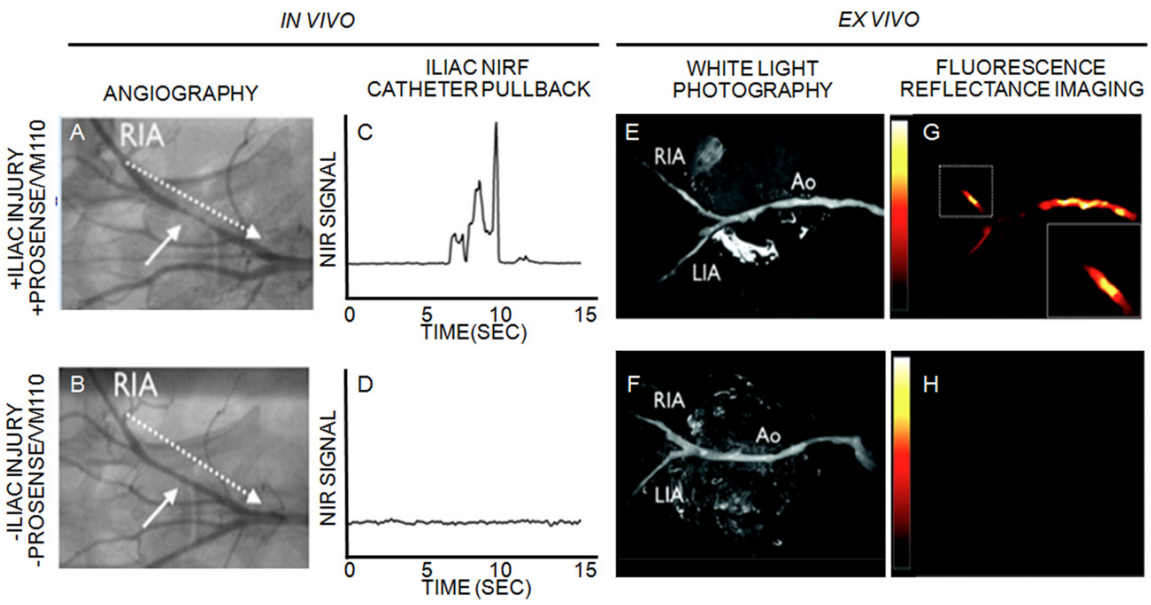

Figure 1. One-dimensional *in vivo* NIRF molecular sensing of cysteine protease activity associated with atheroma. Rabbits undergoing balloon injury of the right internal iliac artery and received the NIRF molecular imaging agent Prosense/VM110 (top row) and saline controls (bottom row) were generated. A, B. Angiography demonstrates a stenosis in the right internal iliac artery of the balloon-injured but not the control animals. Manual pullback of the one-dimensional NIRF catheter was performed (dashed arrow). C, D. One-dimensional *in vivo* mapping of the sensed NIRF signal during manual pullback demonstrates increased signal at the iliac atheroma (solid arrow in A, Prosense/VM110-injected animal) but no signal in the control plaque (solid arrow in B, saline-injected animal). Paired *ex vivo* white light (E and F) and FRI (G and H) confirms that cysteine protease activity localized to atheroma in the injured animals only. FRI, fluorescence reflectance imaging; NIRF, near-infrared fluorescence. Adapted from [30].

cate vulnerable plaques and thus represent high-value targets for atherosclerotic molecular imaging.

Prosense/VM110, a specialized cathepsin-activatable NIRF imaging agent has been developed and validated in a number of preclinical atherosclerotic animal models for imaging of cathepsins B, S, and L [25, 32, 33]. Comprised of an array of 15-20 NIR fluorochromes conjugated to an inert biochemical scaffold (protected graft copolymer spanning a poly-lysine backbone), the intentionally closely spaced fluorochromes result in "self-quenching," resulting in only minimal levels of background signal. Such a feature confers a major advantage over conventional agents that emit signal at the time of injection. The incorporation of oligonucleotide target sequence into the scaffold provides tunable target specificity, for example to cathepsin K [33]. Upon specific interaction with cathepsins *in vivo*, cleavage of the quenched substrate and liberation of the multiple fluorochromes leads to amplified, local NIRF signal [24, 30].

In vivo one-dimensional intravascular NIRF molecular sensing with a first-generation catheter system

As a first step towards developing a clinically useful intravascular NIRF imaging platform to detect atherosclerotic inflammation *in vivo*, in 2008 a first-generation NIRF molecular sensing catheter was constructed and evaluated [30]. This prototype was capable of focal NIR light emission and detection on an area of ~40um diameter and ~2mm from the catheter but was not equipped with automated pullback or rotational capability. Thus, NIRF intravascular detection was constrained to one-dimensional sensing with limited longitudinal anatomical accuracy.

In conjunction with the cathepsin-activatable NIRF probe Prosense/VM110, preliminary studies demonstrated that NIRF signal resulting from localization and then cathepsin-based activation of Prosense/VM110 could be detected *in vivo* in atherosclerotic iliac arteries (<2.5 mm diameter) of balloon-injured, hyperlipid-

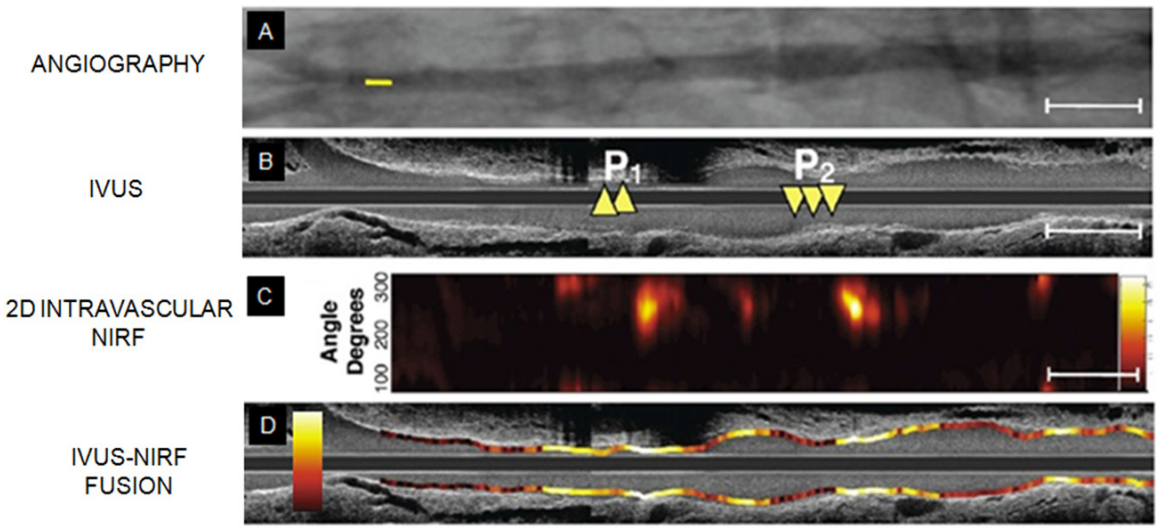

Figure 2. Two-dimensional *in vivo* NIRF molecular imaging of aortic atherosclerotic inflammation. A. Angiography of the iliac bifurcation and distal abdominal aorta in balloon-injured hyperlipidemic rabbits was used to co-register the IVUS images. The tip of the NIRF imaging catheter prior to automated rotation and pullback is indicated (yellow bar). B. Corresponding longitudinal IVUS imaging demonstrates moderate atheroma at positions P1 and P2 (yellow arrows). C. Two-dimensional NIRF imaging aligned with angiographic (A) and IVUS (B) imaging demonstrates high NIRF signal localized to aortic atheroma. D. Longitudinal fused NIRF/IVUS images. For NIRF imaging, yellow/white color denotes strongest intensity NIRF signal; red/black denotes lowest intensity NIRF signal. NIRF, near-infrared fluorescence; IVUS, intravascular ultrasound. Adapted from [24].

emic rabbits (**Figure 1**). Importantly, NIRF signal detection was accomplished through blood, without the need for flushing or occlusion, affirming the favorable light transmission properties of the NIR window. Specifically, one-dimensional line mapping of the sensed NIRF signal assessed by manual pullback demonstrated high signal levels that co-localized with atheroma. In contrast, minimal NIRF signal was detected in atherosclerotic rabbits receiving saline or in those normal rabbits receiving Prosense/VM110. *Ex vivo* fluorescence reflectance imaging (FRI) confirmed the localization of NIRF signal to these injured areas. While demonstrating feasibility, a fully comprehensive 360-degree imaging assessment of arteries was not possible with this system.

In vivo intravascular two-dimensional NIRF molecular imaging with a second-generation catheter system

To address the limitations associated with the one-dimensional NIRF catheter, a new catheter engineered with automated pullback and 360° rotation was constructed [24]. Using NIRF phantoms submerged in a bloodlike solution (1% intralipid and 50ppm India Ink), the catheter imaging performance specifications were determined to be suitable for *in vivo* imaging: specifically, its angular resolution was 35°- 42° with an ability to resolve greater than 8 sectors at a catheter-to-target distance of 3.0mm; its longitudinal z-resolution was 1.0mm at a catheter-to-target distance of 2.0mm.

The *in vivo* NIRF imaging utility of this second-generation two-dimensional catheter was then investigated in the relatively larger rabbit aorta (3-4mm diameter versus 2.25-2.5mm rabbit iliac artery evaluated previously). Eight weeks after sustaining balloon-mediated aortic injury, hyperlipidemic rabbits received Prosense/VM110 or saline. Intravascular ultrasound (IVUS) was performed to more precisely identify the very mild lesions not detectable by conventional angiography. Next, intravascular NIRF molecular aortic imaging (3.5mm diameter vessel), facilitated by both automated pullback and rotational systems, was then performed following conventional angiography. Fusion of the anatomical data afforded by IVUS with the NIRF imaging data demonstrated the localization of NIR signal to aortic atherosclerotic plaques. Specifically, in rabbits with atheromata, the signal-to-noise (SNR) and target-to-background ratios (TBR) were significantly higher in those treated with Prosense/VM110 versus saline

(median [quartiles]: SNR = 12.6 [8.1, 20.6] vs. 1.3 [0.9, 2.1], p-value = 0.02; TBR = 6.3 [4.3, 9.4] vs. 1.1 [0.9, 1.4], p-value = 0.02). Subsequent *ex vivo* studies of the excised aortas corroborated the *in vivo* findings (**Figure 2**). Only those animals sustaining balloon denudation arterial injury and receiving Prosense/VM110 exhibited plaque-associated NIRF signal on *ex vivo* FRI; injured animals that received saline lacked any appreciable aortic NIRF signal (p-value = 0.01). Interestingly, immunostaining and histologic studies of both early and advanced plaques demonstrated that despite the presence of macrophages and cathepsin B staining in both types of lesions, NIRF signal was only appreciably detected in more the advanced, relatively larger plaques. These findings suggest that immature plaques, demonstrating the presence of cathepsin but lacking significant cysteine protease activity, may be less inflamed versus more mature lesions.

Integrated in vivo OFDI/NIRF imaging

The ability to combine NIRF molecular imaging with exactly co-registered structural imaging would represent a major advance. Optical frequency domain imaging (OFDI) is an FDA-approved, high-speed intravascular imaging modality that expands upon the unparalleled anatomic resolution of optical coherence tomography (OCT), offering an axial resolution of ~10-20um. Specifically by post-processing OCT image acquisitions by Fourier transformation, various components of the arterial wall including stents, thrombus, lipid, and calcium can be rendered not only with high levels of spatial resolution but also in two- and three-dimensional representations [34]. As such, the integration of high-resolution OFDI with intravascular NIRF molecular imaging would offer exquisitely precise co-registration of microscopic anatomical imaging with *in vivo* biologic data.

Yoo and Kim *et al.* recently described the development of a catheter capable of simultaneous intravascular dual-modality OFDI/NIRF imaging [22]. This system provided cross-sectional OFDI imaging of vessel microstructural detail with micrometer levels of both axial and transverse resolution (~7 and ~30-um respectively), high frame rate acquisition capability (25.4 frames per second), adequate depth of imaging (4.6mm in saline), and enhanced sensitivity to detect NIR fluorochromes (<1nM). The ability of integrated OFDI/NIRF intravascular imaging to detect inflamed atherosclerotic plaque was then investigated. Using hypercholesterolemic rabbits previously undergoing balloon-mediated iliac arterial injury, Prosense/VM110 was administered 24h prior to combined OFDI/NIRF intravascular assessment. Plaques detected by OFDI were associated with strong NIRF signal while normal appearing arterial regions largely lacked such. Indeed, consistent with the earlier results derived from imaging with the single-modality NIRF imaging catheters, *ex vivo* histologic studies confirmed that the inflamed lesions identified by OFDI/NIRF intravascular imaging were highly enriched with both macrophages and cathepsin B. The highly sensitive microstructural mapping of enhanced proteolytic activity of plaques provided by this imaging platform may then advance the identification of the interrelated structural and biologic features of vulnerable plaque not captured by conventional methods. Additionally, this approach may also greatly accelerate the development of novel therapeutics to treat atherosclerosis by providing a means to longitudinally and non-destructively monitor the effects of investigational agents on plaque inflammation and microstructure.

In vivo NIRF imaging of lipid- and macrophage-enriched atheroma with indocyanine green

While Prosense/VM110 is highly promising for NIRF molecular imaging of inflammation, it is not yet clinically available. Therefore, to accelerate the translation of intravascular NIRF imaging, clinically approved NIRF imaging agents are needed. Indocyanine green (ICG), an amphiphilic NIR fluorochrome approved by the Food and Drug Administration for ophthalmologic NIRF imaging of retinal and choroidal vasculature [35], has previously been shown to bind both low- and high-density lipoproteins [36] as well as accumulate in inflamed tissues [37]. Given these attractive features for atherosclerosis imaging, we explored the ability of ICG to detect lipid-laden atherosclerotic plaques *in vivo* via intravascular NIRF imaging [38]. Initially, 8 weeks following aortic balloon-mediated injury, hyperlipidemic rabbits were administered ICG or saline. *Ex vivo* analyses showed that when compared to hyperlipidemic or uninjured animals receiving saline or ICG respectively, atheroma-bearing animals injected with ICG

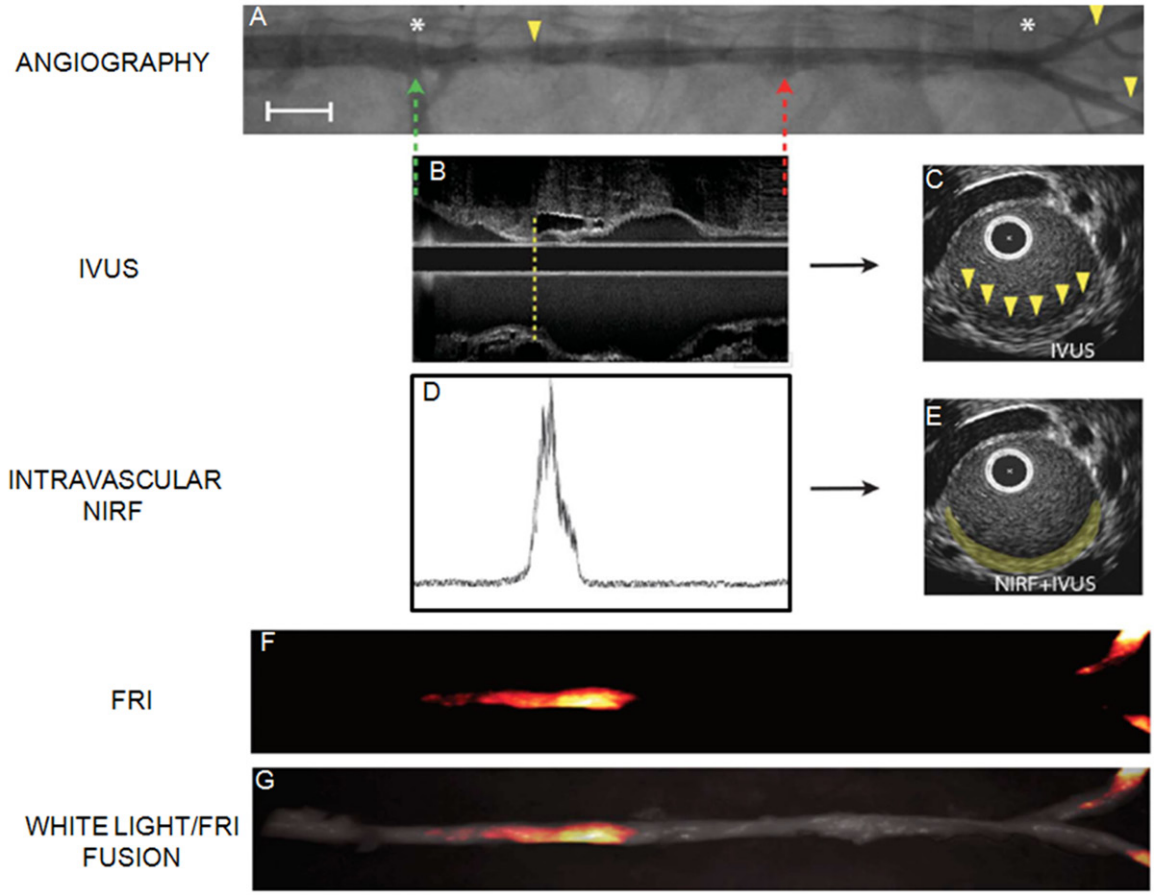

Figure 3. *In vivo* intravascular NIRF imaging of ICG localized to atherosclerotic plaques. A. Angiographic images of the aortic and iliac atherosclerotic lesions (yellow arrowheads). The beginning and end of the automated NIRF catheter pullback are demarcated by the green and red dotted lines respectively. White asterisks indicate arterial branch points that serve as fiduciary markers for co-registration. B, C. Longitudinal IVUS image of the aortic plaque and cross-sectional IVUS image acquired at the position indicated by the yellow dashed line. The aortic atherosclerotic plaque is evident in cross-section (C: yellow arrows). D, E. Maximal NIRF signal acquired on automated distal to proximal pullback with NIRF imaging catheter localizes to the aortic plaque. Fused cross-sectional IVUS and NIRF image demonstrates that NIRF signal (E: shaded yellow) localized to the aortic plaque. F, G. Enhanced NIRF signal is seen in both the aorta and iliac arteries on standalone *ex vivo en face* FRI (F) as well as fused white light photographic-FRI (G). ICG, indocyanine green; FRI, fluorescence reflectance imaging; NIRF, near-infrared fluorescence; IVUS, intravascular ultrasound. Adapted from [38].

demonstrated significant NIRF signal that localized within atheroma. Histological studies demonstrated that ICG deposition co-localized with plaque lipids (neutral triglyceride stained by Oil Red O) and RAM-11 positive macrophages. Adjunctive *in vitro* studies demonstrated that ICG not only bound acetylated LDL, but also was endocytosed by both macrophages and foam cells. Complementary studies with resected human carotid endarterectomy operative specimens incubated with ICG substantiated these findings as ICG largely localized to macrophage- and lipid-rich areas. The overall histological and mechanistic studies support that ICG identifies inflamed, lipid-rich plaques.

The utility of ICG to provide *in vivo* atheroma NIRF enhancement was then evaluated. Atheroma-bearing rabbits received an IV bolus of ICG (1.5mg/kg, an FDA-approved dose) followed by multimodal intravascular imaging and NIRF sensing. As seen in **Figure 3**, utilizing the one-dimensional NIRF intravascular sensing catheter system modified with automated pullback capability, NIRF signal enhancement was detected in aorta and iliac atheroma, as confirmed by co-registered angiographic and intravascular ultrasound (IVUS) anatomical images. *In vivo* NIRF findings were corroborated by fused *ex vivo* white light photography/FRI images. Complementary studies consisting of serial

intravascular NIRF interrogations showed that *in vivo* plaque NIRF signals were durably detected up to 45 minutes following ICG administration.

As an FDA-approved imaging agent, ICG-based NIRF intravascular molecular imaging is a clinically translatable approach to detect inflamed, lipid-laden atherosclerotic plaque *in vivo*. While the mechanistic details governing ICG accumulation in plaques, such as factors determining its uptake by macrophage subsets and other cells as well as its binding to lipid subtypes still requires further elucidation, this study demonstrates the feasibility of targeted NIRF molecular imaging strategies to detect alternative features of vulnerable plaques.

In vivo NIRF imaging of stent-induced inflammatory arterial injury

Stent thrombosis is a relatively uncommon but a frequently fatal complication of percutaneous coronary intervention (PCI), a procedure that is performed over 1 million times a year in the US alone. Occurring in ~0.3-1.0% of patients undergoing PCI annually, stent thrombosis predominantly presents as an acute myocardial infarction typically requiring emergent percutaneous revascularization [39]. The 30-day mortality of patients experiencing stent thrombosis is high (i.e. ~10-25%). Of note, drug-eluting stents (DES), the standard of care for most patients undergoing PCI, may induced impaired healing that leads to a persistent rate of late stent thrombosis. Furthermore, one-fifth of stent thrombosis survivors will experience a recurrent event within 2 years. Given the high morbidity and mortality associated with such, recent clinical investigations have focused upon determining the critical patient and procedural risk factors associated with an increased risk of developing stent thrombosis. Intravascular structural imaging techniques such as IVUS or optical coherence tomography (OCT) remain the mainstay of identifying any inciting mechanical factors (i.e. exposed stent struts, stent malapposition, or stent fracture). However, these studies have not yet allowed precise identification of high-risk stents prone to developing stent thrombosis.

Within the last decade, the underlying biology of stent thrombosis has been elucidated, offering an inroad for molecular imaging of stent biology. Post-mortem histological studies of stented arterial segments from patients implanted with bare metal (BMS) or DES show that the latter stent type is associated with both significantly more delayed healing and uncovered stent struts (reduced endothelialization) [40, 41]. Additionally, the struts of the DES were much more inflamed, with higher levels of inflammatory cells and fibrin deposition seen associated with each strut. Supported by other histologic studies, both uncovered as well as fibrin-associated stent struts have been recognized as important histologic predictors of stent thrombosis [42]. Thus a need exists to more accurately characterize these critical biomolecular aspects of inflammation and fibrin-deposition following PCI with BMS or DES. Importantly, the identification of stents that are persistently inflamed or enriched with fibrin may represent potentially modifiable factors that not only help promote stent thrombosis, but also may be amenable to pharmacologic intervention.

To investigate the ability of intravascular NIRF imaging to sense inflammatory arterial injury and stent healing after PCI, rabbits underwent bare-metal stenting of the aorta following balloon dilatation (**Figure 4**) [24]. Six days after implantation, the animals received Prosense/VM110 and then on the next day underwent angiography, IVUS, and intravascular NIRF imaging. Enhanced NIRF signal was noted at both the proximal and distal edges of the stents suggesting that the interface between the stent-covered and uncovered arterial wall was particularly apt to develop inflammatory injury, possibly due to arterial injury provoked by the edge of the stent. Additionally, enhanced activity was noted several millimeters away from the stent edge and was thought attributable to extension of injury by balloon inflation beyond the stent edges. This study represents a new approach to assess *in vivo* arterial inflammation and healing at high-resolution following stent implantation. Notably, this system offers a method of serial, nondestructive assessment that may better elucidate both the temporal and spatial patterns of inflammatory injury following stenting. Preclinical intravascular NIRF imaging studies could thus better guide interventional procedures to minimize arterial injury, pharmacotherapy to better optimize stent healing and vessel passivation, and better evaluate the bioinflammatory aspects of novel coronary

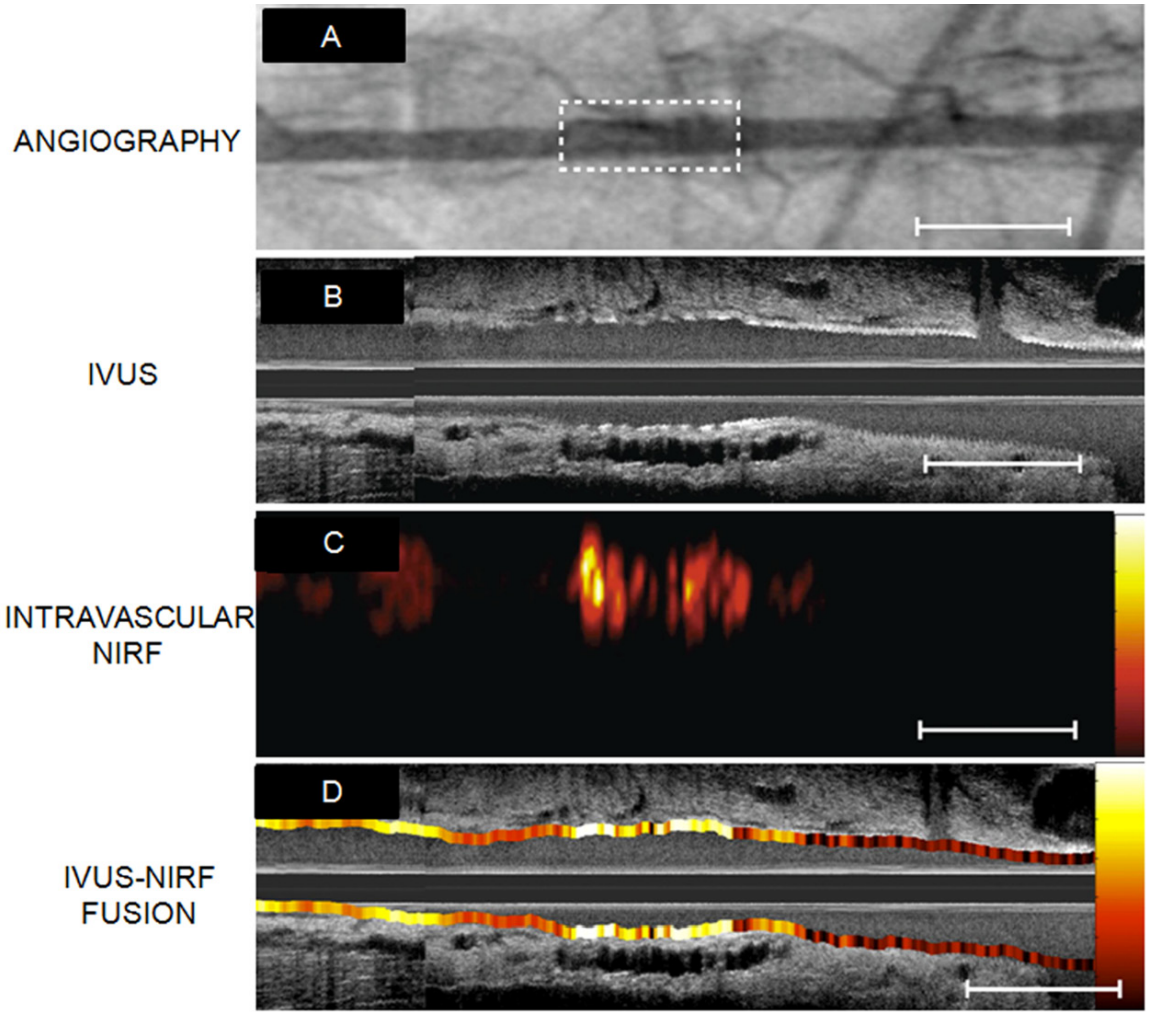

Figure 4. *In vivo* two-dimensional NIRF molecular imaging through blood of inflammatory injury patterns following stent implantation in coronary-sized arteries. A. The dashed box in the angiographic image denotes the position of a stent deployed in the abdominal aorta of hyperlipidemic rabbits. B, C. Facilitated by automated pullback and rotation, longitudinal IVUS images (B) clearly demarcate the exact position of the aortic stent that, from simultaneously acquired NIRF imaging (C), is associated with significantly increased local proteolytic activity. D. The fused longitudinal NIRF/IVUS image (yellow/white color denotes strongest intensity NIRF signal; red/black denotes lowest intensity NIRF signal). NIRF, near-infrared fluorescence; IVUS, intravascular ultrasound. Adapted from [24].

stent designs. Moreover, high-resolution two-dimensional intravascular NIRF imaging, in select clinical scenarios, may offer a useful tool to identify those previously implanted stents at higher risk for developing stent thrombosis (see section entitled "Clinical Trajectory").

In vivo NIRF imaging of stent-associated fibrin deposition

Fibrin deposition on stent struts is implicated in the development of stent thrombosis [42], but limited options are available to specifically image fibrin deposition on stents *in vivo*. To meet this need, we applied intravascular NIRF molecular imaging to detect stent-associated fibrin microthrombi [22]. First, *ex vivo* integrated OFDI/NIRF imaging studies were performed on a NIR fluorescent Cy7-labeled fibrin-coated stent implanted into a cadaveric coronary artery implanted (**Figure 5**). OFDI visualized stent and arterial microstructure including the arterial wall, stent struts, and stent-associated thrombus. Simultaneous NIRF images precisely co-registered by OFDI revealed fibrin-specific NIRF signal mapped onto a subset of the stent-associated thrombus. Subsequent *en face* FRI of the stented artery corroborated these findings. The ability of this system to detect stent-associated fibrin microthrombi *in vivo* was then

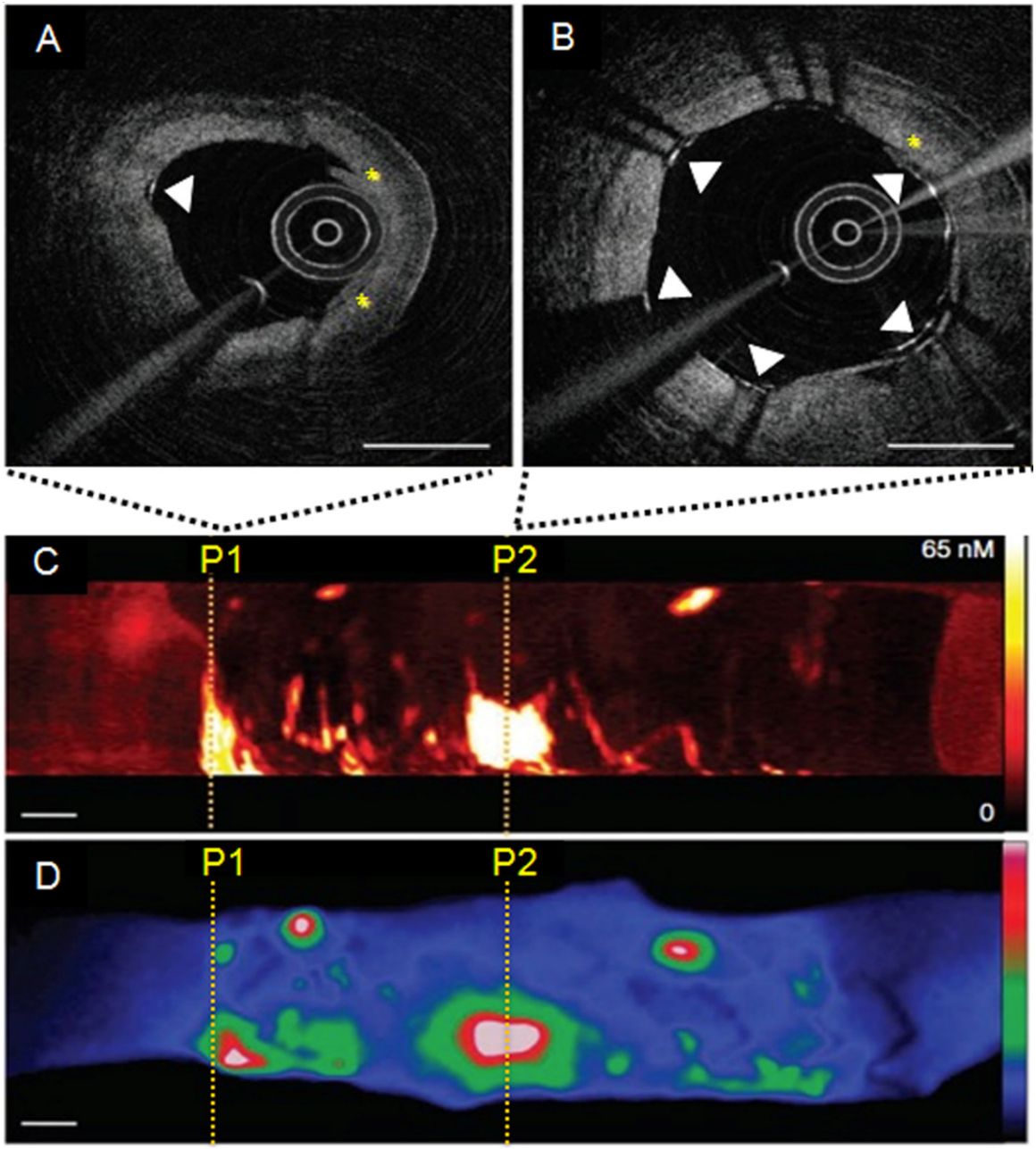

Figure 5. *Ex vivo* OFDI/NIRF imaging of a cadaveric human coronary artery implanted with a stent coated with Cy7-labelled fibrin-targeted nanoparticle. A-D. Microthrombi (yellow asterisks) associated with the stent struts (white arrowheads) are present on cross-sectional OFDI images at positions P1 (A) and P2 (B) that correspond with areas of high intensity NIRF signal on two-dimensional NIRF imaging (C: yellow/white color denotes strongest intensity NIRF signal; red/black denotes lowest intensity NIRF signal) and *ex vivo en face* FRI (D: red/white color denotes strongest intensity fluorescence signal; blue/black denotes lowest intensity fluorescence signal). FRI, fluorescence reflectance imaging; NIRF, near-infrared fluorescence; OFDI, optical frequency domain imaging. Adapted from [22].

studied (**Figure 6**). NIR fluorescent Cy7-labeled fibrin-coated stents were implanted in the iliac artery of a living rabbit followed by imaging using the dual-modality OFDI/NIRF catheter. The stent struts and associated microthrombi were visible by OFDI and, when integrated with NIRF imaging, demonstrated that the NIRF signal co-localized to a portion of the thrombi. Subsequent *ex vivo* microscopic studies demonstrated that NIRF-molecular imaging was

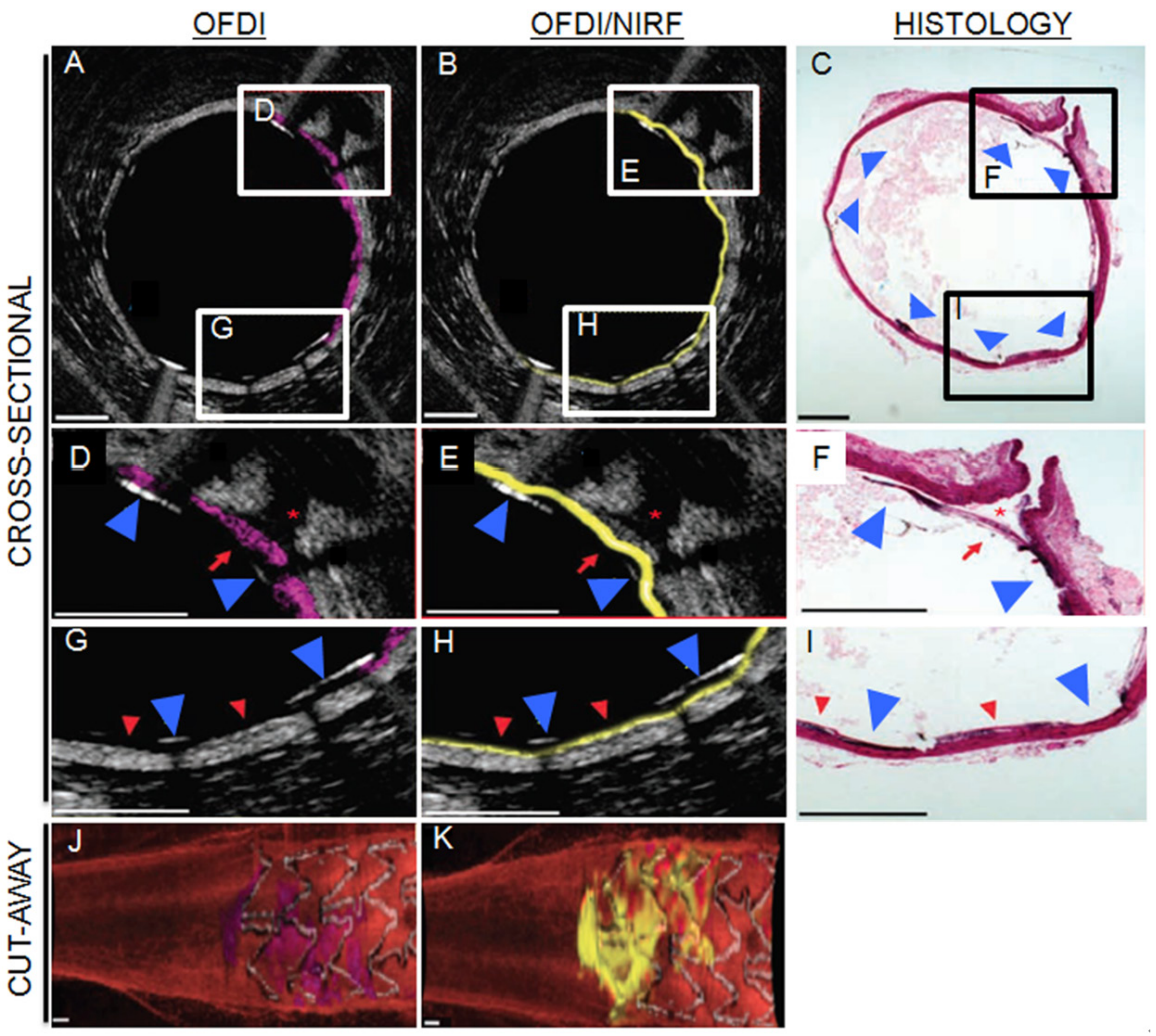

Figure 6. *In vivo* OFDI/NIRF imaging of a Cy7-labelled fibrin-targeted nanoparticle coated stent implanted in rabbit iliac artery. Images derived from standalone OFDI (left panels), integrated OFDI/NIRF (middle panels), and *ex vivo* hematoxylin and eosin histology (*right panels*) are shown. A-C. Cross-sectional OFDI images demonstrate thrombus (A: purple) while OFDI/NIRF fusion images show NIRF signal (B: yellow) that are closely correlated and associated with the stent struts (C: blue arrowheads). D-F. Magnified views confirm that the thrombus (D: purple, demarcated by red arrow; F: demarcated by red arrow) corresponds closely to the pattern of NIRF signal detected (E: yellow, demarcated by red arrow) and confirm the association between the stent struts (blue arrowheads) and thrombus. Additional arterial microstructural details are clearly present such as an arterial side branch (red asterisks). G-I. Areas devoid of thrombus (G: red arrowhead) but are NIRF-positive are detected and correspond to fibrin by histology. J, K. Three-dimensional rendering of the stented right iliac artery *in vivo* (i.e. "cut away" view) demonstrates the NIRF signal localized to the stent-associated thrombus when the standalone OFDI image (J) is compared with the fused OFDI/NIRF image (K). OFDI, optical fluorescence domain imaging; NIRF, near-infrared fluorescence. Adapted from [22].

more sensitive than OFDI for fibrin detection. Ultimately, with the development of injectable of translatable fibrin sensors [43], integrated OFDI/NIRF intravascular imaging may help better assess the future risk of developing stent thrombosis by detecting angiographically unapparent but clinically important stent-associated fibrin microthrombi.

Clinical trajectory

While currently in the preclinical stages of investigation, the enhanced diagnostic capabilities of intravascular NIRF imaging, particularly the dual-modality OFDI/NIRF platform incorporating simultaneous microstructural imaging, may be of substantial clinical utility.

While new insights into the molecular pathophysiology underlying plaque instability and rupture may be realized in the near term, clinical benefits derived from NIRF molecular imaging must demonstrate improved sensitivity/receive-operator curves beyond traditional risk measures (e.g. Framingham risk score and coronary artery calcium scoring). Such a prospect will require a longer term, large event-based clinical trial. NIRF/OFDI imaging may therefore find more immediate clinical utility in identifying stents at risk of stent thrombosis, which occurs more reliably then clinical ruptures of vulnerable plaques (i.e. the PROSPECT trial [44]). Specifically NIRF molecular imaging has the potential to identify at-risk stents by identifying stent-associated fibrin or inflammation. In this way, challenging clinical scenarios such as gauging the potential risk of stent thrombosis attributable to interrupting dual antiplatelet therapy for imminent but non-emergent surgery might be better managed by a combined microstructural-functional interrogation of any previously implanted stents, particularly if they reside in critical, proximal locations. Additionally, protracted healing with persistent inflammation of prior stents in patients hospitalized for acute coronary syndrome may suggest the need for intensified antiplatelet or anticoagulation medical regimens.

Limitations

While intravascular NIRF imaging techniques offer a novel method for assessing the *in vivo* biology of plaques and stented arteries, there are limitations that must be considered. First, intravascular molecular imaging, an invasive technique, would ideally be performed on subgroups of patients already stratified as high-risk by noninvasive risk prediction methods. Additionally, the impact of arterial calcification, coronary arterial tortuosity, and blood flow on autofluorescence and overall sensitivity will need to be evaluated.

Conclusion

Intravascular NIRF molecular imaging of inflammation and microthrombi in atheroma and stent-induced arterial injury is a new translational approach that can offer new biologic insights pertaining to human coronary atherosclerosis. Leading dual-modality approaches such as integrated OFDI/NIRF offers simultaneous high-resolution microstructural co-registration and localization of important *in vivo* biologic signals, which may help identify high-risk plaques and stents at risk of thrombosis. Clinical translation appears promising based on the prototypical intravascular NIRF catheters already developed in conjunction with the emergence of targeted imaging agents [45]. Surpassing traditional angiographic measures of luminal stenosis to critically assess plaque biology and microstructure, it is likely that intravascular NIRF molecular imaging, as a component of a multimodal intravascular imaging approach, will remain at the forefront of atherobiologic imaging in the near future.

Acknowledgements

Funding support from NIH R01 HL108229, MGH SPARK Award, MGH ECOR Award.

Disclosures

FAJ - Research Support, Merck, Abbott Vascular. Consultant, Boston Scientific.

Address correspondence to: Farouc A Jaffer, Massachusetts General Hospital, Harvard Medical School, Cardiovascular Research Center, 185 Cambridge Street, Room 3206, Boston, Massachusetts 02114, USA. Phone: 617-724-9353; Fax: 617-860-3180; E-mail: fjaffer@mgh.harvard.edu

References

[1] Go AS, Mozaffarian D, Roger VL, Benjamin EJ, Berry JD, Borden WB, Bravata DM, Dai S, Ford ES, Fox CS, Franco S, Fullerton HJ, Gillespie C, Hailpern SM, Heit JA, Howard VJ, Huffman MD, Kissela BM, Kittner SJ, Lackland DT, Lichtman JH, Lisabeth LD, Magid D, Marcus GM, Marelli A, Matchar DB, McGuire DK, Mohler ER, Moy CS, Mussolino ME, Nichol G, Paynter NP, Schreiner PJ, Sorlie PD, Stein J, Turan TN, Virani SS, Wong ND, Woo D, Turner MB; American Heart Association Statistics Committee and Stroke Statistics Subcommittee. Heart Disease and Stroke Statistics-2013 Update A Report From the American Heart Association. Circulation 2013 Jan 1; 127: 143-52.

[2] Krumholz HM, Wang Y, Chen J, Drye EE, Spertus JA, Ross JS, Curtis JP, Nallamothu BK, Lichtman JH, Havranek EP, Masoudi FA, Radford MJ, Han LF, Rapp MT, Straube BM and Normand SLT. Reduction in Acute Myocardial In-

farction Mortality in the United States. JAMA 2009; 302: 767-773.
[3] Glagov S, Weisenberg E, Zarins CK, Stankunavicius R and Kolettis GJ. Compensatory Enlargement of Human Atherosclerotic Coronary Arteries. N Engl J Med 1987; 316: 1371-1375.
[4] Virmani R, Burke AP, Farb A and Kolodgie FD. Pathology of the Vulnerable Plaque. J Am Coll Cardiol 2006; 47: C13-C18.
[5] Adamu U, Knollmann D, Alrawashdeh W, Almutairi B, Deserno V, Kleinhans E, Schäfer W and Hoffmann R. Results of Interventional Treatment of Stress Positive Coronary Artery Disease. Am J Cardiol 2010; 105: 1535-1539.
[6] Jaffer FA, Libby P and Weissleder R. Molecular Imaging of Cardiovascular Disease. Circulation 2007; 116: 1052-1061.
[7] Sanz J and Fayad ZA. Imaging of atherosclerotic cardiovascular disease. Nature 2008; 451: 953-957.
[8] Chen IY and Wu JC. Cardiovascular Molecular Imaging. Circulation 2011; 123: 425-443.
[9] Fuster V, Fayad ZA, Moreno PR, Poon M, Corti R and Badimon JJ. Atherothrombosis and High-Risk Plaque: Part II: Approaches by Noninvasive Computed Tomographic/Magnetic Resonance Imaging. J Am Coll Cardiol 2005; 46: 1209-1218.
[10] Virmani R, Burke AP, Farb A and Kolodgie FD. Pathology of the unstable plaque. Prog Cardiovasc Dis 2002; 44: 349-356.
[11] Sukhova GK, Shi GP, Simon DI, Chapman HA and Libby P. Expression of the elastolytic cathepsins S and K in human atheroma and regulation of their production in smooth muscle cells. J Clin Invest 1998; 102: 576-583.
[12] Schmitz SA, Taupitz M, Wagner S, Wolf KJ, Beyersdorff D and Hamm B. Magnetic resonance imaging of atherosclerotic plaques using superparamagnetic iron oxide particles. J Magn Reson Imaging 2001; 14: 355-361.
[13] Schmitz S, Taupitz M, Wagner S, Coupland S, Gust R, Nikolova A and Wolf K. Iron-Oxide-Enhanced Magnetic Resonance Imaging of Atherosclerotic Plaques: Postmortem Analysis of Accuracy, Inter-Observer Agreement, and Pitfalls. Invest Radiol 2002; 37: 405-4011.
[14] Tang TY, Howarth SPS, Miller SR, Graves MJ, Patterson AJ, U-King-Im JM, Li ZY, Walsh SR, Brown AP, Kirkpatrick PJ, Warburton EA, Hayes PD, Varty K, Boyle JR, Gaunt ME, Zalewski A and Gillard JH. The ATHEROMA (Atorvastatin Therapy: Effects on Reduction of Macrophage Activity) Study: Evaluation Using Ultrasmall Superparamagnetic Iron Oxide-Enhanced Magnetic Resonance Imaging in Carotid Disease. J Am Coll Cardiol 2009; 53: 2039-2050.
[15] Rudd JHF, Warburton EA, Fryer TD, Jones HA, Clark JC, Antoun N, Johnström P, Davenport AP, Kirkpatrick PJ, Arch BN, Pickard JD and Weissberg PL. Imaging Atherosclerotic Plaque Inflammation With [18F]-Fluorodeoxyglucose Positron Emission Tomography. Circulation 2002; 105: 2708-2711.
[16] Tawakol A, Migrino RQ, Bashian GG, Bedri S, Vermylen D, Cury RC, Yates D, LaMuraglia GM, Furie K, Houser S, Gewirtz H, Muller JE, Brady TJ and Fischman AJ. In Vivo 18F-Fluorodeoxyglucose Positron Emission Tomography Imaging Provides a Noninvasive Measure of Carotid Plaque Inflammation in Patients. J Am Coll Cardiol 2006; 48: 1818-1824.
[17] Fayad ZA, Mani V, Woodward M, Kallend D, Abt M, Burgess T, Fuster V, Ballantyne CM, Stein EA, Tardif JC, Rudd JHF, Farkouh ME and Tawakol A. Safety and efficacy of dalcetrapib on atherosclerotic disease using novel non-invasive multimodality imaging (dal-PLAQUE): a randomised clinical trial. The Lancet 2011; 378: 1547-1559.
[18] Dunphy MPS, Freiman A, Larson SM and Strauss HW. Association of Vascular 18F-FDG Uptake with Vascular Calcification. J Nucl Med 2005; 46: 1278-1284.
[19] Cheng VY, Slomka PJ, Le Meunier L, Tamarappoo BK, Nakazato R, Dey D and Berman DS. Coronary Arterial 18F-FDG Uptake by Fusion of PET and Coronary CT Angiography at Sites of Percutaneous Stenting for Acute Myocardial Infarction and Stable Coronary Artery Disease. J Nucl Med 2012; 53: 575-583.
[20] Saam T, Rominger A, Wolpers S, Nikolaou K, Rist C, Greif M, Cumming P, Becker A, Foerster S, Reiser M, Bartenstein P and Hacker M. Association of inflammation of the left anterior descending coronary artery with cardiovascular risk factors, plaque burden and pericardial fat volume: a PET/CT study. Eur J Nucl Med Mol Imaging 2010; 37: 1203-1212.
[21] Wykrzykowska J, Lehman S, Williams G, Parker JA, Palmer MR, Varkey S, Kolodny G and Laham R. Imaging of Inflamed and Vulnerable Plaque in Coronary Arteries with 18F-FDG PET/CT in Patients with Suppression of Myocardial Uptake Using a Low-Carbohydrate, High-Fat Preparation. J Nucl Med 2009; 50: 563-568.
[22] Yoo H, Kim JW, Shishkov M, Namati E, Morse T, Shubochkin R, McCarthy JR, Ntziachristos V, Bouma BE, Jaffer FA and Tearney GJ. Intra-arterial catheter for simultaneous microstructural and molecular imaging in vivo. Nat Med 2011; 17: 1680-1684.
[23] Jaffer FA, Libby P and Weissleder R. Optical and Multimodality Molecular Imaging: Insights Into Atherosclerosis. Arterioscler Thromb Vasc Biol 2009; 29: 1017-1024.
[24] Jaffer FA, Calfon MA, Rosenthal A, Mallas G, Razansky RN, Mauskapf A, Weissleder R, Libby

P and Ntziachristos V. Two-Dimensional Intravascular Near-Infrared Fluorescence Molecular Imaging of Inflammation in Atherosclerosis and Stent-Induced Vascular Injury. J Am Coll Cardiol 2011; 57: 2516-2526.

[25] Chen J, Tung CH, Mahmood U, Ntziachristos V, Gyurko R, Fishman MC, Huang PL and Weissleder R. In Vivo Imaging of Proteolytic Activity in Atherosclerosis. Circulation 2002; 105: 2766-2771.

[26] Sosnovik DE, Nahrendorf M, Deliolanis N, Novikov M, Aikawa E, Josephson L, Rosenzweig A, Weissleder R and Ntziachristos V. Fluorescence Tomography and Magnetic Resonance Imaging of Myocardial Macrophage Infiltration in Infarcted Myocardium In Vivo. Circulation 2007; 115: 1384-1391.

[27] Nahrendorf M, Jaffer FA, Kelly KA, Sosnovik DE, Aikawa E, Libby P and Weissleder R. Noninvasive Vascular Cell Adhesion Molecule-1 Imaging Identifies Inflammatory Activation of Cells in Atherosclerosis. Circulation 2006; 114: 1504-1511.

[28] Olson ES, Whitney MA, Friedman B, Aguilera TA, Crisp JL, Baik FM, Jiang T, Baird SM, Tsimikas S, Tsien RY and Nguyen QT. In vivo fluorescence imaging of atherosclerotic plaques with activatable cell-penetrating peptides targeting thrombin activity. Integr Biol 2012; 4: 595-605.

[29] Jaffer FA, Tung CH, Gerszten RE and Weissleder R. In Vivo Imaging of Thrombin Activity in Experimental Thrombi With Thrombin-Sensitive Near-Infrared Molecular Probe. Arterioscler Thromb Vasc Biol 2002; 22: 1929-1935.

[30] Jaffer FA, Vinegoni C, John MC, Aikawa E, Gold HK, Finn AV, Ntziachristos V, Libby P and Weissleder R. Real-Time Catheter Molecular Sensing of Inflammation in Proteolytically Active Atherosclerosis. Circulation 2008; 118: 1802-1809.

[31] Liu J, Sukhova GK, Sun JS, Xu WH, Libby P and Shi GP. Lysosomal Cysteine Proteases in Atherosclerosis. Arterioscler Thromb Vasc Biol 2004; 24: 1359-1366.

[32] Aikawa E, Nahrendorf M, Sosnovik D, Lok VM, Jaffer FA, Aikawa M and Weissleder R. Multimodality Molecular Imaging Identifies Proteolytic and Osteogenic Activities in Early Aortic Valve Disease. Circulation 2007; 115: 377-386.

[33] Jaffer FA, Kim DE, Quinti L, Tung CH, Aikawa E, Pande AN, Kohler RH, Shi GP, Libby P and Weissleder R. Optical Visualization of Cathepsin K Activity in Atherosclerosis With a Novel, Protease-Activatable Fluorescence Sensor. Circulation 2007; 115: 2292-2298.

[34] Tearney GJ, Waxman S, Shishkov M, Vakoc BJ, Suter MJ, Freilich MI, Desjardins AE, Oh WY, Bartlett LA, Rosenberg M and Bouma BE. Three-Dimensional Coronary Artery Microscopy by Intracoronary Optical Frequency Domain Imaging. JACC Cardiovasc Imaging 2008; 1: 752-761.

[35] Stanga PE, Lim JI and Hamilton P. Indocyanine green angiography in chorioretinal diseases: indications and interpretation: An evidence-based update. Ophthalmology 2003; 110: 15-21.

[36] Yoneya S, Saito T, Komatsu Y, Koyama I, Takahashi K and Duvoll-Young J. Binding properties of indocyanine green in human blood. Invest Ophthalmol Vis Sci 1998; 39: 1286-1290.

[37] Fischer T, Gemeinhardt I, Wagner S, Stieglitz Dv, Schnorr J, Hermann KGA, Ebert B, Petzelt D, MacDonald R, Licha K, Schirner M, Krenn V, Kamradt T and Taupitz M. Assessment of Unspecific Near-Infrared Dyes in Laser-Induced Fluorescence Imaging of Experimental Arthritis. Acad Radiol 2006; 13: 4-13.

[38] Vinegoni C, Botnaru I, Aikawa E, Calfon MA, Iwamoto Y, Folco EJ, Ntziachristos V, Weissleder R, Libby P and Jaffer FA. Indocyanine Green Enables Near-Infrared Fluorescence Imaging of Lipid-Rich, Inflamed Atherosclerotic Plaques. Sci Transl Med 2011; 3: 84ra45.

[39] Holmes DR Jr, Kereiakes DJ, Garg S, Serruys PW, Dehmer GJ, Ellis SG, Williams DO, Kimura T and Moliterno DJ. Stent Thrombosis. J Am Coll Cardiol 2010; 56: 1357-1365.

[40] Joner M, Finn AV, Farb A, Mont EK, Kolodgie FD, Ladich E, Kutys R, Skorija K, Gold HK and Virmani R. Pathology of Drug-Eluting Stents in Humans: Delayed Healing and Late Thrombotic Risk. J Am Coll Cardiol 2006; 48: 193-202.

[41] Nakazawa G, Finn AV, Joner M, Ladich E, Kutys R, Mont EK, Gold HK, Burke AP, Kolodgie FD and Virmani R. Delayed Arterial Healing and Increased Late Stent Thrombosis at Culprit Sites After Drug-Eluting Stent Placement for Acute Myocardial Infarction Patients. Circulation 2008; 118: 1138-1145.

[42] Finn AV, Joner M, Nakazawa G, Kolodgie F, Newell J, John MC, Gold HK and Virmani R. Pathological Correlates of Late Drug-Eluting Stent Thrombosis. Circulation 2007; 115: 2435-2441.

[43] Hara T, Bhayana B, Thompson B, Kessinger CW, Khatri A, McCarthy JR, Weissleder R, Lin CP, Tearney GJ and Jaffer FA. Molecular Imaging of Fibrin Deposition in Deep Vein Thrombosis Using Fibrin-Targeted Near-Infrared Fluorescence. JACC Cardiovasc Imaging 2012 Jun; 5: 607-15.

[44] Stone GW, Maehara A, Lansky AJ, de Bruyne B, Cristea E, Mintz GS, Mehran R, McPherson J, Farhat N, Marso SP, Parise H, Templin B, White R, Zhang Z and Serruys PW. A Prospective Nat-

ural-History Study of Coronary Atherosclerosis. N Engl J Med 2011; 364: 226-235.

[45] van Dam GM, Themelis G, Crane LMA, Harlaar NJ, Pleijhuis RG, Kelder W, Sarantopoulos A, de Jong JS, Arts HJG, van der Zee AGJ, Bart J, Low PS and Ntziachristos V. Intraoperative tumor-specific fluorescence imaging in ovarian cancer by folate receptor-[alpha] targeting: first in-human results. Nat Med 2011; 17: 1315-1319.